Int. J. Electrochem. Sci., 10 **(2015)** 5827 - 5841

International Journal of
ELECTROCHEMICAL
SCIENCE
www.electrochemsci.org

Effect of Heat Treatment on Mechanical Property and Electrochemical Corrosion Behavior of X65 Pipeline Steel in 3.5 wt.% NaCl

Hongwei Wang[1,*], *Chi Yu*[2], *Shaowen Huang*[3]

[1] School of Information Science & Engineering, Northeastern University, Shenyang 110819, China;
[2] School of Materials and Metallurgy, Northeastern University, Shenyang 110819, China
[3] Laiwu Iron and Steel Group Company Limited, Laiwu 271100, China
[*]E-mail: wanghw0819@163.com

Received: 10 April 2015 / *Accepted:* 29 April 2015 / *Published:* 27 May 2015

The effect of heat treatment on the mechanical property and electrochemical corrosion behavior of X65 pipeline steel in 3.5 wt.% NaCl solution (pH=3.5) is investigated. The study is carried out using tensile test, impact test, potentiodynamic polarization and electrochemical impedance spectroscopy measurements. The results show that the pipeline steel at tempering temperature 300^{o}C has good mechanical property, but the pipeline steel at tempering temperature 650^{o}C has good corrosion resistance performance. The mutual relationship of tempering temperature, microstructure, mechanical property and electrochemical corrosion behavior are discussed.

Keywords: pipeline steel; heat treatment; mechanical property; electrochemical corrosion behavior

1. INTRODUCTION

The local corrosion of pipeline steel is extremely complex because numerous factors, such as metallurgical, geometrical and environmental, will together contribute to this corrosion process [1]. The pipeline steel not only requires good mechanical properties, but also has excellent corrosion resistance. So it is essential to develop pipeline steel and study the mechanical property and corrosion behavior.

Heat treatment is propitious to reduce the internal defect. Recently, it has been found that pipeline steel after heat treatment exhibits good mechanical properties, with high tensile strength and good ductility. Many researchers have focused significant attention, got some results [2-6]. In fact, these steel are exposed to the special corrosion environment. And a few papers have been devoted to

the corrosion behavior of pipeline steel [7-10]. Therefore, the corrosion problem of pipeline steel has very important research significance.

Now, the electrochemical measurement method is a powerful tool for researching corrosion process, the technology has been widely used to investigate the corrosion mechanism and has been proven to be effective. They have obtained many good results [11-17]. As is well known, few studies have been reported in the literature concerning the mutual relationship tempering temperature, microstructure, electrochemical measurements of pipeline steel under strong solution [7, 18-20].

In this paper, we investigate the effect of heat treatment on the mechanical property and electrochemical corrosion behavior of pipeline steel under strong acid NaCl solution. Firstly, the microstructures are observed by optical microscope (OM) and scanning electron microscopy (SEM). Then, the polarization curve and electrochemical impedance spectroscopy (EIS) are obtained to analyze the corrosion behavior, and using Tafel fitting and equivalent circuit method, respectively. Finally, the mutual relationship of tempering temperature, microstructure and electrochemical measurements are discussed, which can provide the basic theoretical reference for developing pipeline steel.

2. EXPERIMENTAL MATERIAL AND PROCEDURES

2.1 Materials

A new kind of pipeline steel is made by a vacuum induction melting method based on the idea of low-carbon, high-manganese, and adding some alloy elements for improving mechanical property and corrosion resistance. The chemical composition of low alloy steel is listed in Table 1.

Table 1. Chemical compositions of pipeline steel (mass fraction, wt. %)

C	Si	Mn	P	S	Cu	Ni	Nb	Al	Ti	Ca	Mo
0.053	0.20	1.10	0.008	0.002	0.06	0.15	0.051	0.007	0.015	0.0015	0.16

The steel is fabricated by 50kg vacuum induction melting. The steel ingots are heated to 1100 ^{o}C holding for 30 minutes, and water cooling. After water-quenching, the samples are obtained for different tempering temperature, for 300 ^{o}C, 450 ^{o}C and 650 ^{o}C, are denoted as T300, T450 and T650, respectively, and holding for 1 hour. The microstructures of pipeline steel are observed by OM and SEM.

2.2 Mechanical property tests

The round tensile specimens are diameter of 8mm and original gauge length of 25mm in transverse direction, which are measured by 5105-SANS electronic universal testing machine. The

standard dimension of impact specimens with charpy V-notch specimens are 10mm×10mm×55mm, which are performed on JBW-500 screen display impact testing machine, and the impact tests are performed at room temperature.

2.3 Electrochemical measurements

The electrochemical measurements are performed using a PATSTAT2273 electrochemical workstation. The samples are cut into 10mm×10mm×3mm, and the exposed surface is 10mm×10mm, with an area of 100 mm^2, all other surfaces are isolated from the environment by epoxy resin. Prior to testing, the samples are ground with a series of SiC waterproof abrasive papers (100, 600, 800, 1200 and 1500), washed with acetone and ethanol ultrasonic, and then dried in the air. The experiments are carried out in a conventional three-electrode cell, the platinum electrode as the auxiliary electrode, the saturated calomel electrode (SCE) as the reference electrode, which is connected to the acidic NaCl solution via a Luggin capillary and a salt bridge, and the sample as the working electrode. All polarization curves are recorded potentiodynamic with a scan rate of 1mV/s. Potential sweeps are conducted in the potential range -800 to -500mV(SCE), and a CorrWiew software is used to analyze the polarization curves. The electrochemical impedance spectroscopy experiments are carried out at open circuit voltage using alternating current voltage amplitude of 8mV and a frequency range is from 100 kHz to 0.1 Hz, and Zsimpwin software is used to analyze the EIS results based on an equivalent circuit method. The measurement are performed in 3.5 % (mass fraction) NaCl acidic solution, the PH value of the solution is adjusted to 3.5 using hydrochloric acid solution, the temperature is controlled at about 30℃by electro-thermostatic water bath heating.

3. RESULTS AND DISCUSSION

3.1 Microstructures

Microstructures of the experimental steels are shown in Fig.1. As indicated in Fig.1 (a), it can be seen that the microstructure of T300 steel is typically tempered martensite and banite. Comparing the SEM images in Fig.1(b), it can be found that as follows. Fig.1(c) and (d) show the microstructure of T450 steel, it is mainly composed of lath ferrite and banite, the width of lath ferrite is increased, the fine M/A island disperses in the boundary of ferrite lath grains. The microstructure of T650 steel is composed of polygonal ferrite and small amount of bainite. With the increase of tempering temperature, the ferrite grain sizes get bigger, the bainite grain sizes become smaller.

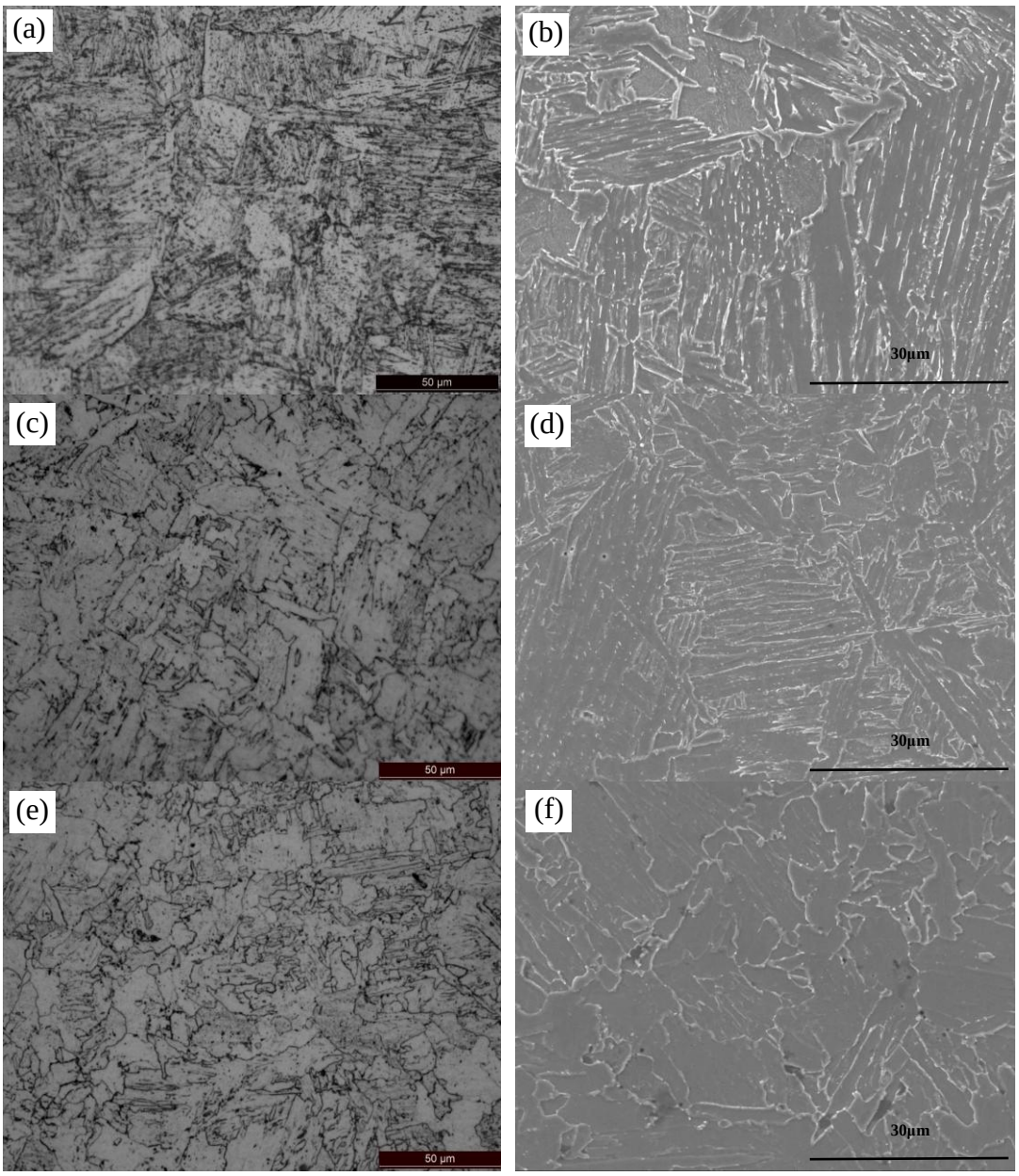

Figure 1. OM images and SEM images of pipeline steel after different tempering temperatures (OM: (a) 300 ^{o}C (c) 450 ^{o}C (e) 650 ^{o}C SEM: (b) 300 ^{o}C (d) 450 ^{o}C (f) 650 ^{o}C)

3.2 Mechanical properties

The tensile strength tests and impact tests are shown in Table 2. It could be clearly seen that the yield strength is between 560 MPa and 620 MPa, and the tensile strength is between 590 MPa and 720 MPa, the elongation is greater than 20%. T650 has the lowest yield strength and tensile strength, but it has the biggest elongation percentage value to be 24.3%. The maximum yielding strength and tensile strength can be obtained for T300 steel. The impact energy range is from 220J to 250J. Based on above analysis, all pipeline steels demonstrate the good mechanical properties.

Table 2. Tensile strength and impact results

Sample	Yield strength /MPa	Tensile strength/MPa	Elongation/%	Impact toughness/J
T300	620	717	23.3	236
T450	601	626	23.8	223
T650	565	597	24.3	246

3.3 Polarization measurements

The potentiodynamic polarization measurement is conducted on the samples after different immersion time. The typical polarization curves for the samples in aerated 3.5 wt% acid NaCl solution are indicated in Fig. 2. The anodic and cathodic branches show Tafel behavior. So Tafel extrapolation can be applied to calculate the corrosion kinetics parameters. The corresponding anodic potential (b_a), cathodic potential (b_c), corrosion potential (E_{corr}), and corrosion current density (I_{corr}) are given in Table 3. All these polarization curves have similar shapes in anodic and cathodic branches, which show that the similar mechanism for corrosion reaction. However, the shape of the cathodic portion varies greatly with the increase the immersion time, which indicates corrosion inhibition basically is the result of decreasing cathodic reaction rate. The corrosion rate v is calculated by substituting corrosion current density taken from Tafel plot for the following equation [21].

$$v = 0.00327\frac{ai}{nD} \qquad (1)$$

where a is molar mass of steel (g/mol), i is corrosion current density ($\mu A/cm^2$), n is valency, D is steel density. It is seen that the high corrosion current density represents big corrosion rate, it will be more prone to corrosion, and vice versa. The corrosion current density of T650 steel is smaller than other steel, and the corrosion current density (I_{corr}) is from 0.0242mA to 0.0265mA, increasing about 0.0023mA. However the changes of the corrosion current density of steels T300 and T450 are relatively fast, the increase values are about 0.0047mA and 0.038mA, respectively. The polarization resistance (R_p) value for steel corrosion is calculated from the Stern-Geary equation [22-24] using parameter listed in Table 3 as follows.

$$R_p = \frac{1}{I_{corr}}\left(\frac{b_c \cdot b_a}{2.3\times(b_c + b_a)}\right) \qquad (2)$$

Based on the above analysis, it is seen that the smallest corrosion current density is observed at immersion time for 96h and the largest one is observed at immersion time for 48h. It may be because the protective films become more stably at immersion time for 96h, which will prevent the steel against corroding substrate further and improve the corrosion resistance. T650 steel shows the good corrosion characteristics, indicating the smaller corrosion current density and the bigger the R_p value. It shows the corrosion rate depends on the steel microstructure, which may be result from the different tempering temperature.

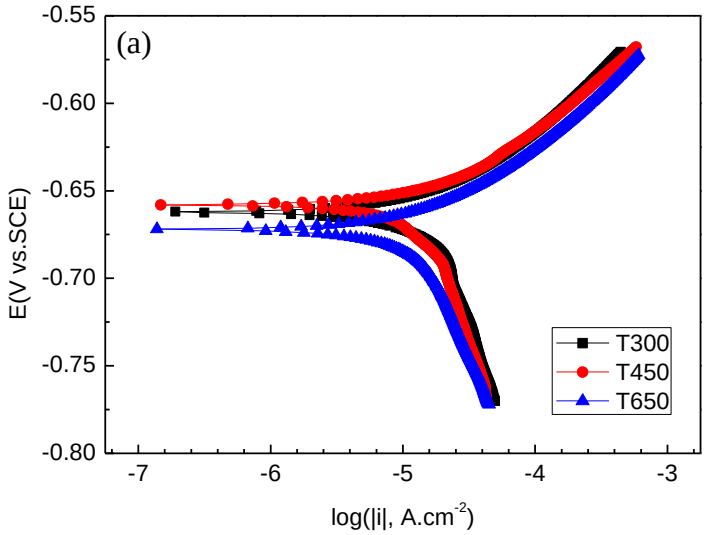
(a)
E(V vs.SCE)
log(|i|, A.cm-2)
T300
T450
T650

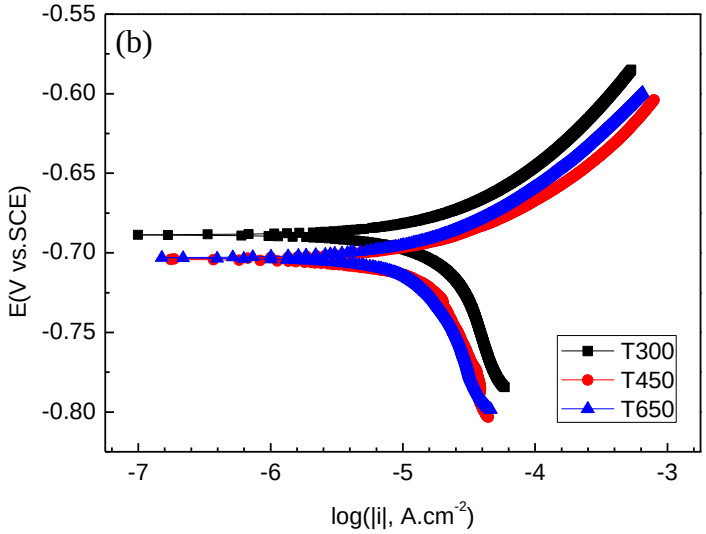
(b)
E(V vs.SCE)
log(|i|, A.cm-2)
T300
T450
T650

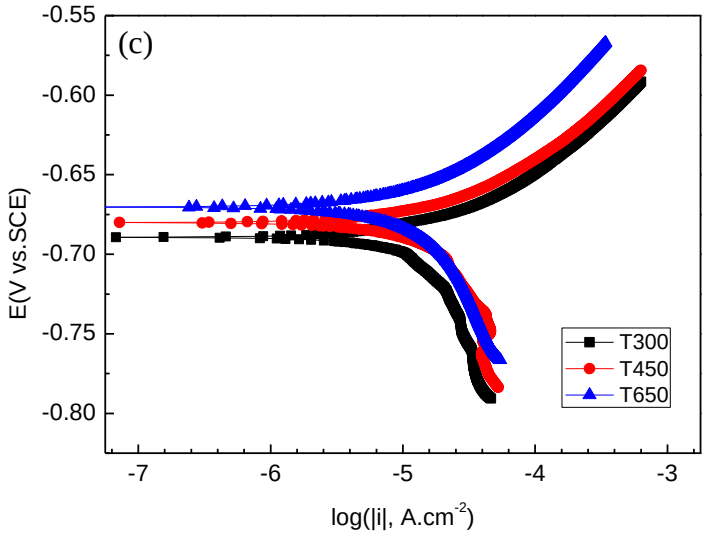
(c)
E(V vs.SCE)
log(|i|, A.cm-2)
T300
T450
T650

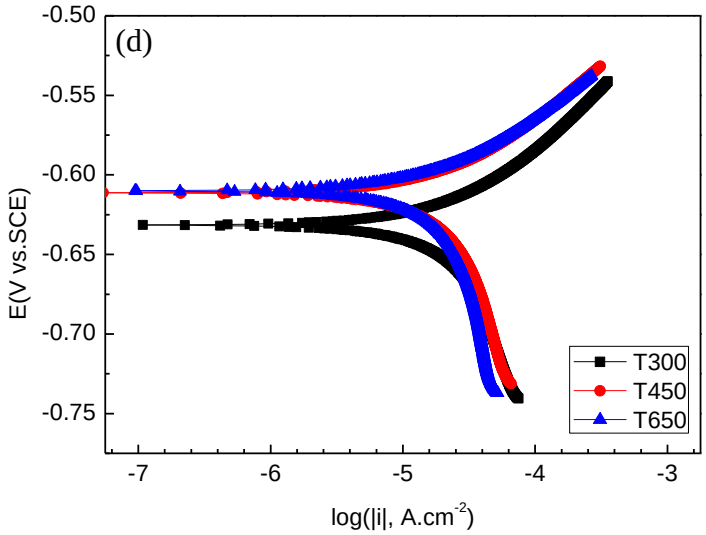

Figure 2. Potentiodynamic polarization curves of pipeline steel (a) bare steel (b) immersion 48 hours (c) immersion 96 hours (d) immersion 168 hours

Table 3. Potentiodynamic polarization parameters from a curve-fitting approach

immersion time/hour	sample	b_a(mV/dec)	b_c(mV/dec)	E_{corr}(V vs.SCE)	I_{corr}(mA.cm^{-2})	R_p($\Omega \cdot cm^2$)
0	T300	77	832	-0.662	0.0326	940
	T450	65	820	-0.658	0.0270	970
	T650	68	502	-0.672	0.0242	1076
48	T300	94	4822	-0.689	0.0504	795
	T450	68	1963	-0.704	0.0341	838
	T650	76	1884	-0.701	0.0325	977
96	T300	72	2619	-0.689	0.0335	909
	T450	71	1562	-0.680	0.0313	943
	T650	90	356	-0.670	0.0263	1188
168	T300	89	414	-0.632	0.0373	854
	T450	77	415	-0.612	0.0308	917
	T600	69	510	-0.610	0.0265	997

3.4 Electrochemical impedance spectroscopy (EIS)

Electrochemical impedance spectroscopy (EIS) is an excellent technique that has been used in analyzing corrosion behavior and corrosion mechanism of metals and alloys in their surrounding environments. The advantage of EIS is its ability to obtain information on corrosion processes that occur on the electrode surface. For a better understanding the effect of immersion time and

microstructure on corrosion behavior of the low alloy steel in sodium chloride solution, the electrochemical impedance spectroscopy (EIS) measurement is performed under the same experimental conditions as the polarization curves. Fig.3 and Fig.4 show the typical Nyquist plots and Bode diagrams for bare pipeline steel samples.

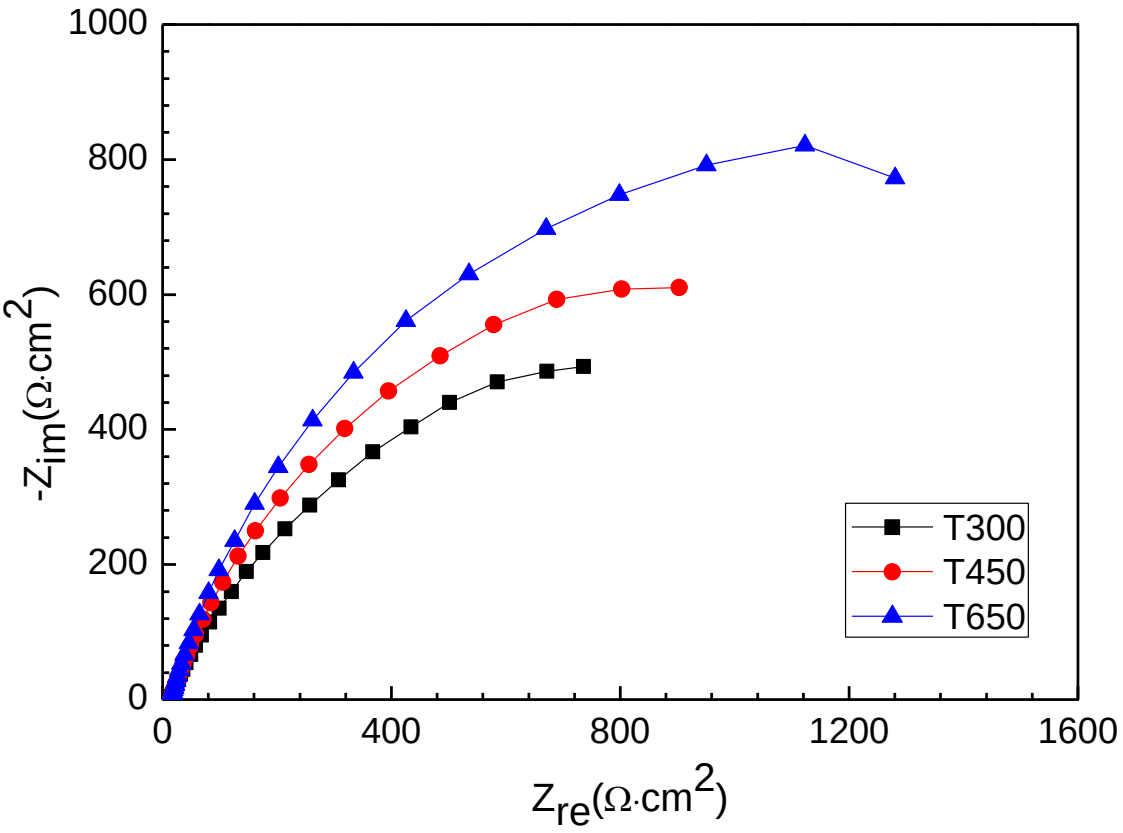

Figure 3. Nyquist plots of bare pipeline steel in 3.5 wt.% NaCl acid solution

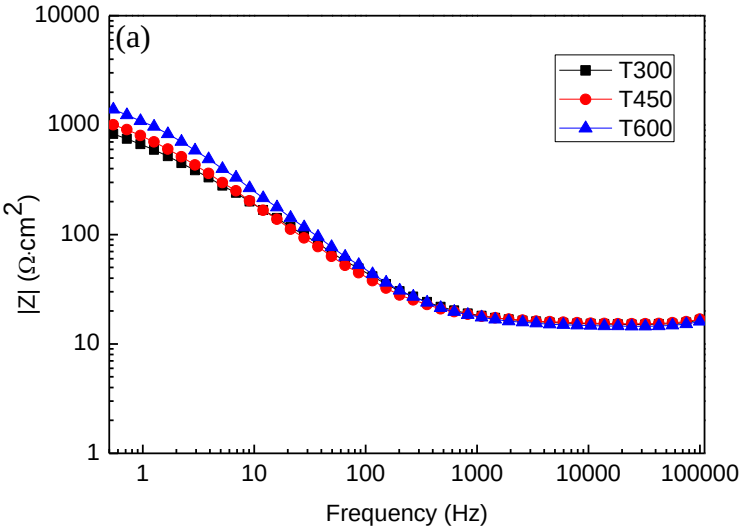

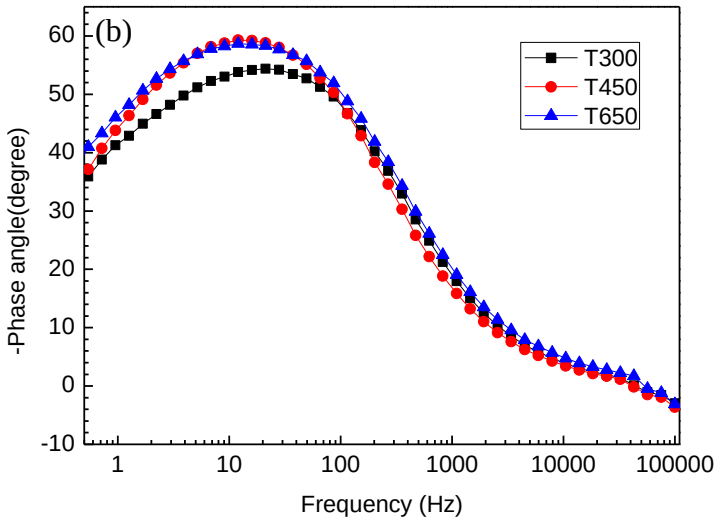

Figure 4. Bode diagrams of the bare pipeline steel in 3.5 wt.% NaCl acid solution (a) The amplitude-frequency characteristic curve (b) The phase-frequency characteristic curve

It is seen that each spectrum includes an incomplete semicircle, the semicircle diameters of T650 steel is larger than steels T300 and T450, the impedance modulus $|Z|$ of pipeline steel will gradually bigger with the increase tempering temperature, and the impedance modulus $|Z|$ is biggest for T650 steel, and the smallest one is for T300 steel in the low frequency range, which will indicate that the corrosion resistance of T650 steel is higher than other steel. The data obtained from Fig.3 is best fitted to the equivalent circuit model depicted in Fig.5. The symbols of the equivalent circuit can be defined according to usual convention as following: Rs represents the electrolyte resistance. CPE is the constant phase element with impedance given by $Z_{CPE}^{-1}=Y_0(j\omega)^n$, where Y_0 is a general admittance function equal to the capacitance C, j is the complex operator with $j=(-1)^{1/2}$, $\omega=2\pi f$ is the angular frequency, n is a power, which is an adjustable parameter that lies between 0 and 1. R_p is the polarization resistance. W is the Warburg impedance with impedance given by $Z_w^{-1}=\sigma\sqrt{j\omega}$, where σ is the Warburg capacitance depending on the diffusion coefficient and the surface concentration of oxidized and reduced species.

The dates are obtained from the equivalent circuits, which are listed in Table 4.

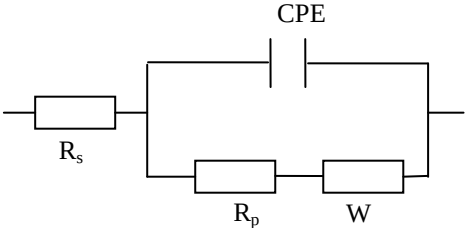

Figure 5. An equivalent circuits with one time constant

Table 4. Fitting values of the equivalent circuit in Fig.5 for bare steel samples in 3.5 wt.% NaCl acid solution

sample	$R_s(\Omega \cdot cm^2)$	$Y_0(F\,cm^{-2})$	n	$R_p(\Omega \cdot cm^2)$	σ $(\Omega^{-1}cm^{-2}s^{0.5})$
T300	14.99	0.0002207	0.7487	833	0.001015
T450	15.40	0.0002066	0.7757	1332	0.001321
T650	14.59	0.0001422	0.7992	1813	0.001318

In order to clarify the corrosion process, the typical Nyquist plots and Bode diagrams of the pipeline steel after different immersion (48, 96 and 168 hours)are displayed in Fig.6 and Fig.7, respectively. Nyquist plots are characterized by only one capacitive arc above the real axis, and the radius of the capacitive arcs is biggest for the steel after immersion 96 hours.

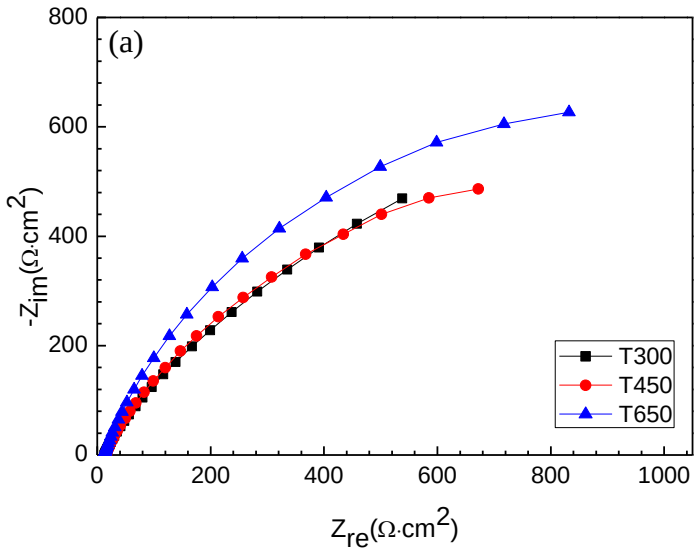

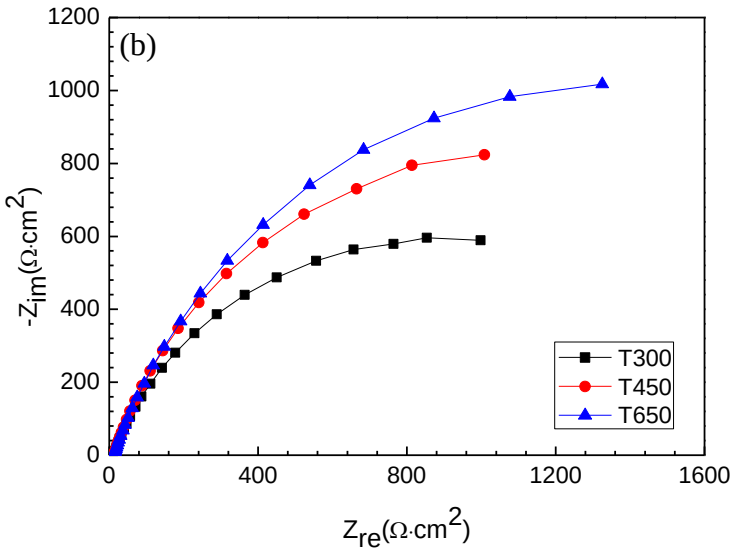

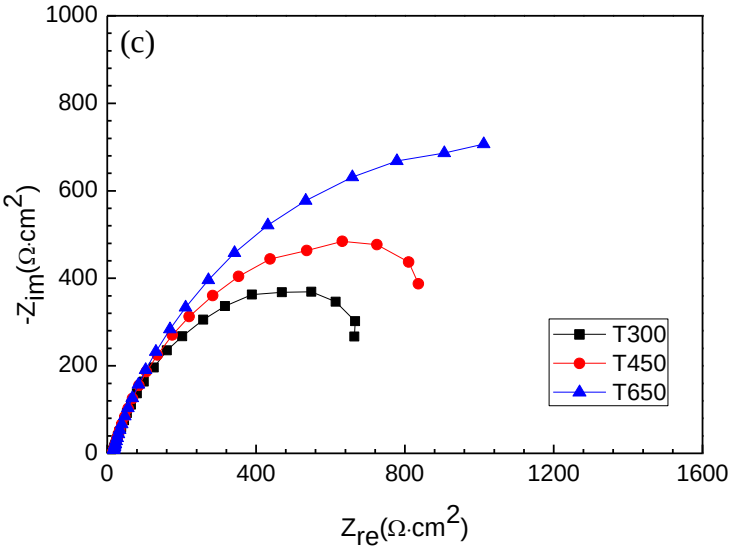

Figure 6. Nyquist plots of pipeline steel after different immersion hours in 3.5 wt.% NaCl acid solution (a) 48 hours (b) 96 hours (c) 168 hours

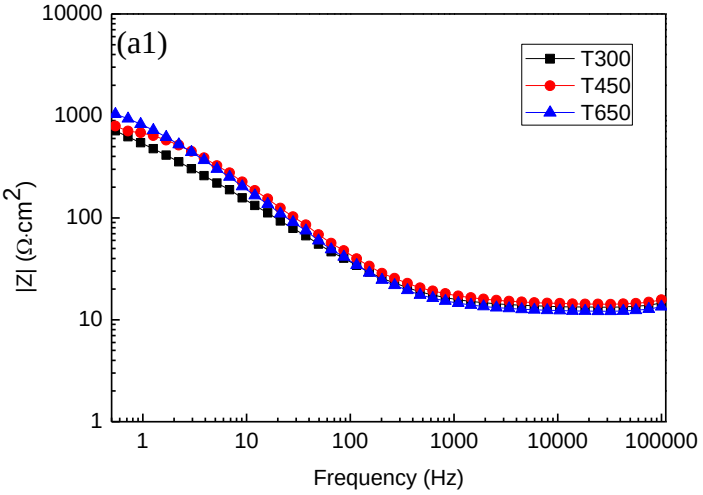

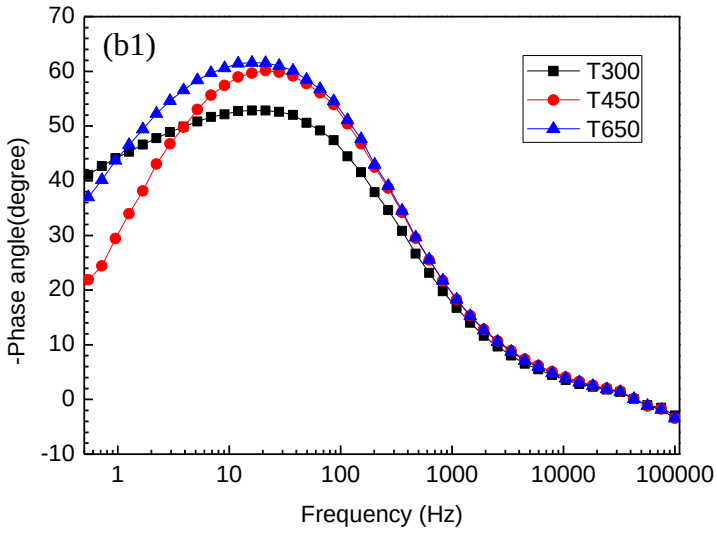

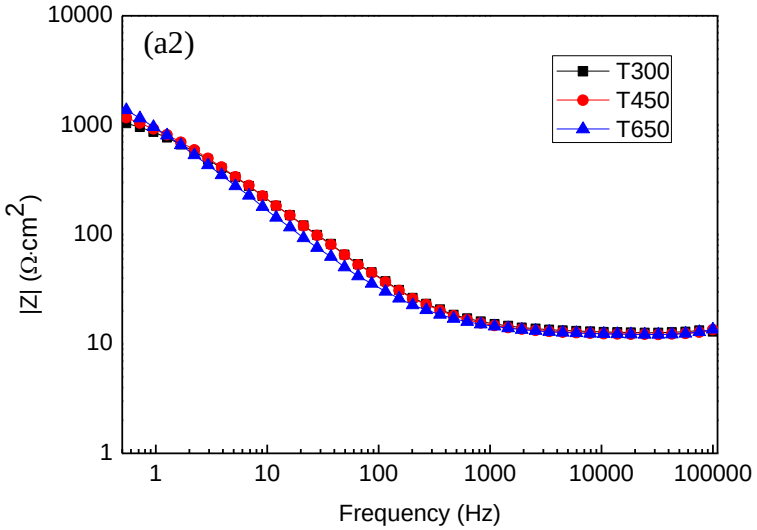
(a2)
T300
T450
T650
|Z| (Ω·cm2)
Frequency (Hz)
10000
1000
100
10
1
1
10
100
1000
10000
100000

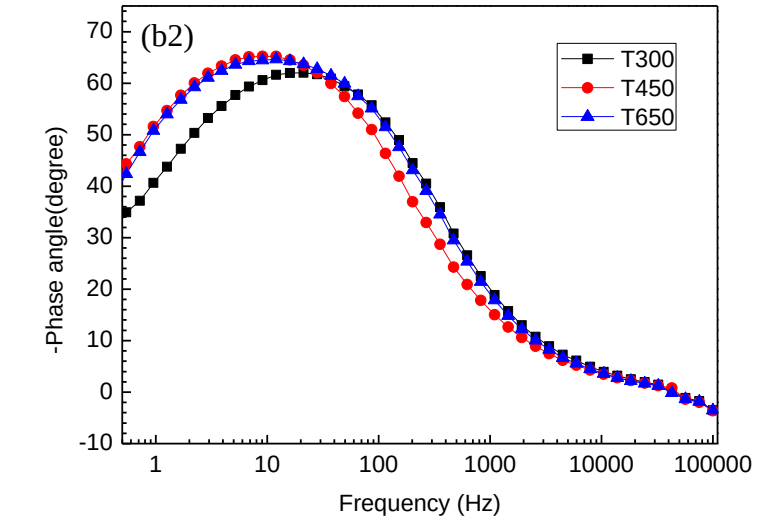
(b2)
T300
T450
T650
-Phase angle(degree)
Frequency (Hz)
70
60
50
40
30
20
10
0
-10
1
10
100
1000
10000
100000

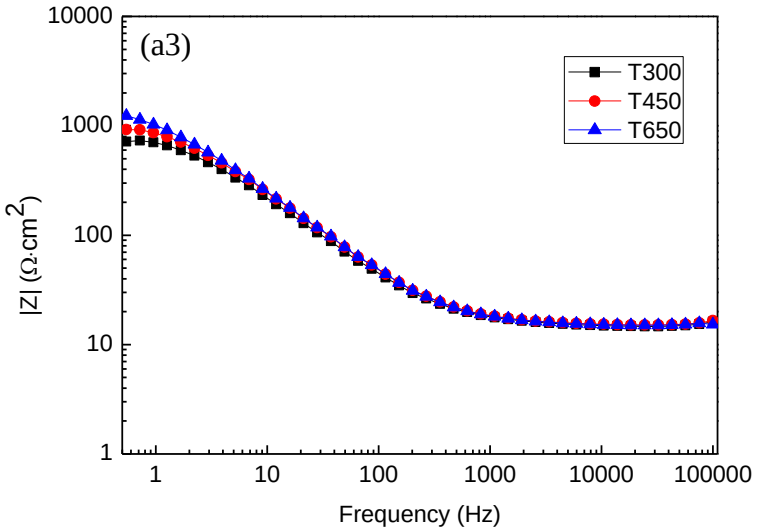
(a3)
T300
T450
T650
|Z| (Ω·cm2)
Frequency (Hz)
10000
1000
100
10
1
1
10
100
1000
10000
100000

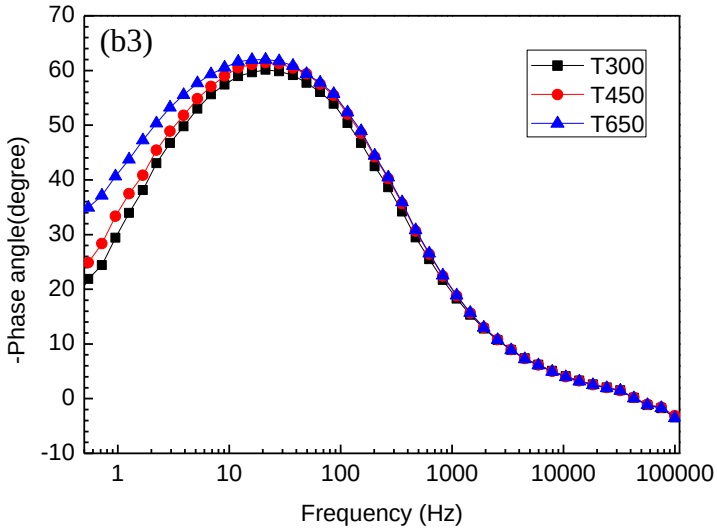

Figure 7. Bode diagrams of pipeline steel after immersion 168 hours in 3.5 wt.% NaCl acid solution (a) The amplitude-frequency characteristic curve (b) The phase-frequency characteristic curve (a1and b1-immersion 48 hours; a2and b2-immersion 96 hours; a3and b3-immersion168hours)

Table 5. Fitting values of the equivalent circuit in Fig.5 for pipeline steel after different immersion hours in 3.5 wt.% NaCl acid solution

Immersion time/hours	sample	$R_s(\Omega\cdot cm^2)$	$Y_0(F\,cm^{-2})$	n	$R_p(\Omega\cdot cm^2)$	σ $(\Omega^{-1}cm^{-2}s^{0.5})$
48	T300	13.24	0.0002898	0.7404	640	0.0008334
	T450	14.40	0.0001628	0.7969	871	0.006314
	T650	12.95	0.0001907	0.7930	1326	0.001275
96	T350	12.71	0.0001659	0.8000	1254	0.001421
	T450	12.55	0.0002332	0.8047	2248	0.007599
	T650	12.80	0.0001793	0.7989	2757	0.005259
168	T300	14.86	0.0001576	0.7968	774	0.004666
	T450	15.25	0.0001364	0.8051	1119	0.002517
	T650	15.07	0.0001388	0.8011	1456	0.001059

In Fig6(c), the arc contraction phenomenon is appeared for steels T300 and T450 after immersion 168 hours, it may be occur the pitting corrosion. It is seen that the impedance modulus $|Z|$ will gradually increase with the increase tempering temperature from Fig.7. The equivalent circuit mode is the same as that shown in Fig.5. The dates are obtained from the equivalent circuits, which are listed in Table 5.

To validate the effectiveness of the fitting dates, the relative residual errors for the real and imaginary components of the impendence (η_{re} and η_{im}) can be calculated using equations (3) and (4), respectively. The residual errors can give a method for understanding the quality of the fit obtained.

$$\eta_{re} = \left(\frac{Z_{re,\exp} - Z_{re,fit}}{Z_{re,\exp}} \right) \times 100\% \quad (3)$$

$$\eta_{im} = \left(\frac{Z_{im,\exp} - Z_{im,fit}}{Z_{im,\exp}} \right) \times 100\% \quad (4)$$

where $Z_{re,\exp}$ and $Z_{im,\exp}$ are the real and imaginary impedances measured from the EIS experimental results, respectively. $Z_{re,fit}$ and $Z_{im,fit}$ are the real and imaginary impedances obtained from the equivalent circuit. The errors with the exception of the highest frequency point are within 5%, which shows the quality of fits is very good, the choice of the equivalent circuit is reasonable.

Based on the above analysis for Table4 and Table 5, R_s value changes a little, the average value is about 13, and the electrolyte resistance is almost the same, which will explain each test system is in a state of relative stability. The values of polarization resistance R_p increase with increase the tempering temperature, thus indicating high resistance of pipeline steel to the corrosive solution. The higher R_p value is obtained for T650 steel after different immersion period, which shows that corrosion resistance of T650 steel is much better than other steels. Compared with the Table 3, the shape of the R_p value is consistent with the polarization curves measurements.

4. CONCLUSIONS

The microstructure, mechanical property and electrochemical corrosion behavior of pipeline steel with varying tempering temperature have been investigated. The conclusions are as follows:

1) With increase tempering temperature, the yielding strength and tensile strength will decrease, the elongation percentage value will increase. The mechanical properties of all samples can meet the standard of pipeline steel, which indicated that the designed process is feasible.

2) The T650 steel with higher tempering temperature exhibits good corrosion resistance with a lower corrosion current density and bigger polarization resistance that steel T300 and T450. At the same time, the protective films become more stably for pipeline steel after immersion time 96h, which will prevent the steel against corroding substrate further and improve the corrosion resistance.

References

1. F.P. Ijsseling, *Corros. J.,* 24 (1989) 55.
2. M. Alizadeh, S. Bordbar, *Corros. Sci.,* 70 (2013) 170.
3. E. M. Sherif, A. A. Almajid, K. A. Khalil, H. Junaedi, F. H. Latief, *Int. J. Electrochem. Sci.,* 8 (2013) 9360.
4. F. Hayat, H. Yzun, *J. Iron. Steel. Res. Int.,* 18(2011)65.
5. J. Liu, H. Yu, Z. Tao, *Mater. Sci. Eng.A,* 619 (2014)212.
6. H. S. Ren, X. J. Tian, H. M. Wang, *Mater. Sci. Eng.A,* 614 (2014)207.
7. E. M. Sherif, A A Almajid, *Int.J.Electrochem.Sci.,* 10(2015)34.
8. L. Y. Xu, Y. F. Cheng, *Corros.Sci.,* 59(2012)103.
9. M. Liu, J. Q. Wang, W. Kei, E. H. Han, *J. Mater. Sci. Technol.,* 30(2014)504.
10. Z. F. Yin, W. Z. Zhao, Z. Q. Bai, Y. R. Feng, W. J. Zhou, *Electrochim. Acta*., 53(2008)3690.
11. Y. Zou, J. Wang, Y. Y. Zheng, *Corros.Sci.*, 53(2011)208.

12. X. L. Zhou, L. Nie, X. Z. Hua, Z. Y. Liu, X. Cui, *J. Chin, Soc. Corros. Prot.,* 32(2012) 423.
13. S. Marcelin, N. Pébère, S. Régnier, *Electrochim. Acta,* 87(2013) 32.
14. S. W. Kim, H. W. Lee, *Int.J.Electrochem.Sci.,* 9(2014) 4709.
15. C. Yu, P. Wang, X. H. Gao, H. W. Wang, *Int.J.Electrochem.Sci.,* 10(2015)538.
16. R. Orinakova, A. Orinak, M. Kupkova, *Int.J.Electrochem.Sci.,* 9(2014) 4268.
17. X. M. Yu, Y. L. Huang, W. J. Qu, *Int.J.Electrochem.Sci.*,9(2014)3760.
18. F. F. Eliyan, E. S. Mahdi, A. Alfantazi, *Corros.Sci.,* 58(2012)181.
19. H. W. Wang, C. Yu, S. X. Wang, J. Gao, *Int.J.Electrochem.Sci.,* 10(2015)1169.
20. X. H. Wang, X. H. Tang, L. W. Wang, C. Wang, Z. Z. Guo, *Int. J. Electrochem. Sci.,* 9(2014)4574.
21. M. N. Ilman, *Eng. Fail. Anal.,* 2(2014)1.
22. E.M. Sherif and S.-M. Park, *Electrochim. Acta,* 51 (2006) 6556.
23. E.M. Sherif and S.-M. Park, *Electrochim. Acta,* 51 (2006) 4665.
24. E.M. Sherif and S.-M. Park, *Corros. Sci.,* 48 (2006) 4065.